which might proceed as a "cage" reaction on the surface of ice. Alternatively, reaction 1 may take place on the ice surface as a concerted, one-step process.

It is also remarkable that substantial quantities of OF_2 are produced when fluorine is passed over cold ice, but not when it is passed into liquid water.[5] We can only conjecture that on the surface of ice it may be possible for relatively large concentrations of F_2 and HOF to build up, allowing the two to interact before either can react with the solvent, whereas in liquid water the steady-state concentrations of F_2 and HOF are too low to permit reaction 1 to proceed to any appreciable extent. The formation of OF_2 from passage of fluorine over H_5IO_6 or hydrated alkali fluorides may have a similar explanation. It is interesting that $KF{\cdot}2H_2O$ is more effective than ice for producing OF_2.

It is well-known, of course, that fluorine does react with aqueous alkali to produce OF_2 in good yield.[5] This suggests possible involvement of the OF^- anion. We have not attempted to address this question in our present study, but we hope to take it up in a future investigation.

In conclusion, therefore, though we have succeeded in identifying the stoichiometric reaction that is responsible for the production of OF_2 from fluorine and water, a great deal of the "why" of this reaction remains shrouded in mystery.

Acknowledgment. We thank Professor Richard C. Thompson of the University of Missouri-Columbia and Professor Robert E. Connick of the University of California, Berkeley for their continuing interest and helpful discussions. We are particularly indebted to Professor Connick for the suggestion that an isotopic tracer experiment might identify the reaction that produces OF_2. We thank Milan Oselka for carrying out the cyclotron irradiations and James Frogge for effecting transport of the fluorine-18 samples. Dr. Irshad Ahmad provided considerable assistance and advice in the setting up of a coincidence counter for fluorine-18. A.W.J. acknowledges the support of a Faculty Research Leave Appointment at Argonne.

Registry No. F_2, 7782-41-4; H_2O, 7732-18-5; O_2, 7782-44-7; HOF, 14034-79-8; OF_2, 7783-41-7; H_2O_2, 7722-84-1.

New Mechanistic Probes of Hydride Abstraction from Rhenium–Alkyl Complexes $(\eta^5\text{-}C_5H_5)Re(NO)(PPh_3)(R)$ by $Ph_3C^+PF_6^-$; Evidence for Initial Electron Transfer

Gerardo S. Bodner,[1a] J. A. Gladysz,*[1a] Merete Folmer Nielsen,[1b] and Vernon D. Parker*[1b]

Contribution from the Department of Chemistry, University of Utah, Salt Lake City, Utah 84112, and Institute for Organic Chemistry, Norwegian Institute of Technology, University of Trondheim, 7034 Trondheim-NTH, Norway. *Received August 1, 1986*

Abstract: The mechanism of hydride abstraction from rhenium–alkyl complexes R–(Re) ((Re) = $(\eta^5\text{-}C_5H_5)Re(NO)(PPh_3)$) by $Ph_3C^+PF_6^-$ is probed by study of the equilibrium R–(Re) + $Ph_3C^+ \rightleftarrows$ R–(Re)$^{\bullet+}$ + $Ph_3C^\bullet$ (eq v) and the effect of oxygen on the rate and deuterium kinetic isotope effect. Equilibrium constants K_5 are determined in CH_2Cl_2 at 208 K from reversible potential measurement for R = $PhCH_2$ (**1**, 2.5×10^{-5}), $(CH_3)_2CHCH_2$ (**2**, 7.9×10^{-3}), and $Ph(CH_3)CH$ (**3**, 5.0×10^{-2}). When generated electrochemically in separate experiments, R–(Re)$^{\bullet+}$ and $Ph_3C^\bullet$ are stable under the reaction conditions. Upon mixing CH_2Cl_2 solutions of the reactants in (v), rapid reactions ensue giving Ph_3CH and hydride abstraction products derived from R–(Re). Thus, if an electron transfer mechanism is operative, very rapid hydrogen atom exchange must take place between R–(Re)$^{\bullet+}$ and $Ph_3C^\bullet$ to displace the unfavorable equilibria (v) to the right. Nearly diffusion controlled rate constants are found for the reaction between $Ph_3C^\bullet$ and O_2, suggesting that $Ph_3C^\bullet$ formed in (v) could be trapped by O_2 and diverted from the pathway leading to Ph_3CH. Rate enhancements of ca. an order of magnitude are observed when reactions are carried out in the presence of oxygen, while the rhenium products are essentially unchanged. A deuterium kinetic isotope effect, k_H/k_D = 5.4, is found for reactions of $PhCH_2$–(Re) and $PhCD_2$–(Re) under nitrogen but not in the presence of oxygen. This indicates that in the presence of O_2 rate control switches from hydrogen atom transfer to electron transfer. In the presence of O_2, as much as 70% of the organic product is benzophenone, arising from decomposition of Ph_3COOH. It is concluded that hydride transfer from R–(Re) to $Ph_3C^+PF_6^-$ most likely takes place by an initial electron transfer followed by hydrogen atom transfer to either $Ph_3C^\bullet$ or $Ph_3COO^\bullet$, depending upon whether O_2 is present.

Transition-metal–alkene complexes are frequently prepared by β-hydride abstraction from alkyl complexes $L_nMCH_2CH_2R$, L_nMCH_2CHRR', or $L_nMCHR'CH_2R$ by the trityl cation (Ph_3C^+), as shown in eq i.[2] Surprisingly, when rhenium–alkyl

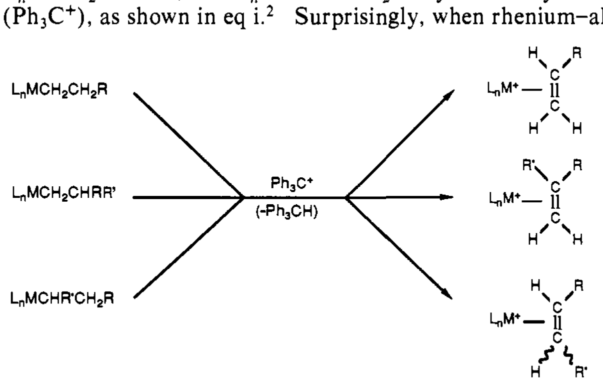

(i)

complexes of the formula $(\eta^5\text{-}C_5H_5)Re(NO)(PPh_3)(CH_2CH_2R)$ (R = H or alkyl) are treated with $Ph_3C^+PF_6^-$, α-hydride abstraction to give *alkylidene* complexes of the formula $[(\eta^5\text{-}C_5H_5)Re(NO)(PPh_3)({=}CHCH_2R)]^+PF_6^-$ rapidly occurs (eq ii).[3-6] However, with rhenium–alkyl complexes of the formulas

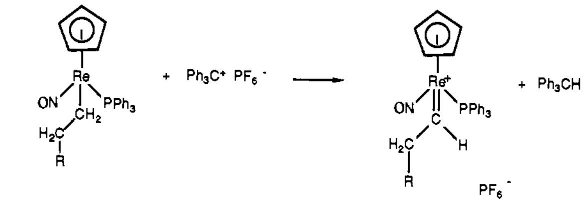

(ii)

(1) (a) University of Utah. (b) University of Trondheim.

(2) See, inter alia: (a) Green, M. L. H.; Nagy, P. L. *J. Organomet. Chem.* **1963**, *1*, 58. (b) Sanders, A.; Cohen, L.; Giering, W. P.; Kenedy, D.; Magatti, C. V. *J. Chem. Soc.* **1973**, *95*, 5430. (c) Cohen, L.; Giering, W. P.; Kenedy, D.; Magatti, C. V.; Sanders, A. *J. Organomet. Chem.* **1974**, *65*, C57. (d) Laycock, D. E.; Hartgerink, J.; Baird, M. C. *J. Org. Chem.* **1980**, *45*, 291. (e) Mink, R. I.; Welter, J. J.; Young, P. R.; Stucky, G. D. *J. Am. Chem. Soc.* **1979**, *101*, 6928.

0002-7863/87/1509-1757$01.50/0

(η^5-C_5H_5)Re(NO)(PPh_3)(CH_2CHRR') or (η^5-C_5H_5)Re(NO)(PPh_3)($CHR'CH_2R$), $Ph_3C^+PF_6^-$ effects a more conventional β-hydride abstraction to give alkene complexes (eq iii and iv).[5]

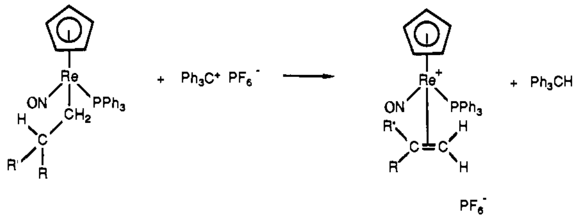

(iii)

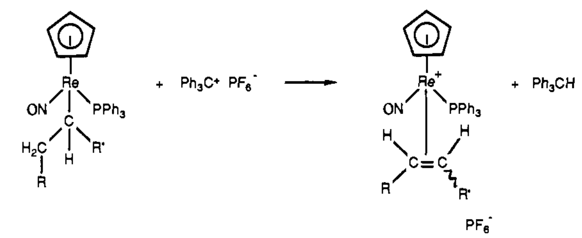

(iv)

Since both α and β C–H bond activation of metal–alkyl intermediates (and the microscopic reverses) are key steps in a variety of catalytic reactions,[7] it is important to understand the mechanistic basis for the α/β-hydride abstraction regiochemistry in these well-defined stoichiometric reactions.

It was originally proposed that an initial Ph_3C^+/(η^5-C_5H_5)Re(NO)(PPh_3)(R) (R–(Re)) electron-transfer step, as shown in eq v, might play a key role in determining the regiochemistry of these reactions.[5,6] Subsequently, it was shown that α-hydride

$$\mathrm{R{-}(Re)} + \mathrm{Ph_3C^+} \overset{K_5}{\rightleftharpoons} \mathrm{R{-}(Re)^{\bullet+}} + \mathrm{Ph_3C^{\bullet}} \qquad (v)$$

abstraction from tungsten–alkyl complexes (η^5-C_5H_5)$_2$W(CH_3)(CH_2R) by $Ph_3C^+PF_6^-$ occurs exclusively by an electron-transfer mechanism.[8] Very recently, paramagnetic intermediates have been detected in the abstraction of an α-hydride from iron–hydroxymethyl complex (η^5-C_5Me_5)Fe(CO)$_2$(CH_2OH) by $Ph_3C^+PF_6^-$[9] and in the abstraction of hydride from 1,3-cyclohexadienyl ligands in (η^6-C_6H_6)Fe(η^4-C_6H_7R) complexes by $Ph_3C^+PF_6^-$.[10] Several (η^5-C_5H_5)Fe(CO)$_2$(CH_2R)/Ph_3C^+ systems have also been probed for electron transfer.[11] Some redox properties of R–(Re) complexes have been reported,[12] but the data were inconclusive regarding the possibility of electron transfer in the hydride abstraction reactions.

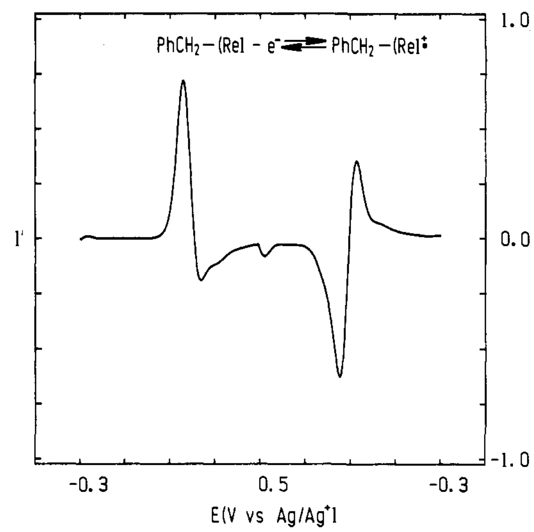

Figure 1. Derivative cyclic voltammogram (DCV) for the oxidation of $PhCH_2$–(Re) (**1**) in $CH_2Cl_2/Bu_4N^+PF_6^-$ (0.1 M) at 208 K and 100 mV/s.

In this paper, we describe electrochemical studies on rhenium–alkyl complexes belonging to each of the three categories exemplified by eq ii–iv:[13] $PhCH_2$–(Re) (**1**),[4] $(CH_3)_2CHCH_2$–(Re) (**2**),[5] and (*SR*,*RS*)-Ph(CH_3)CH–(Re) (**3**).[5] We also use elec-

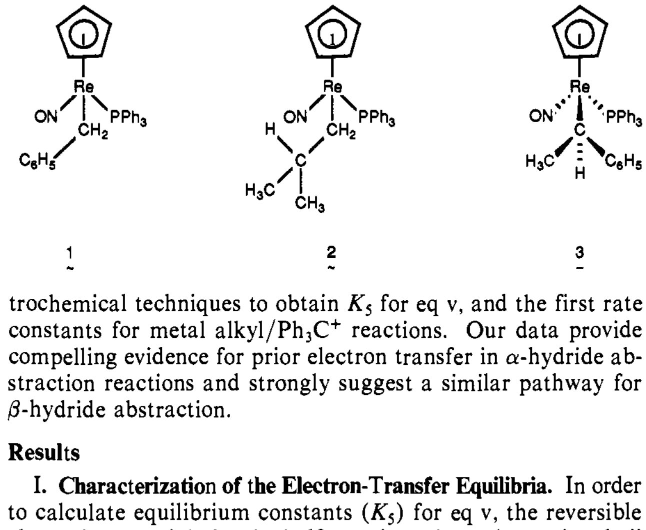

1 2 3

trochemical techniques to obtain K_5 for eq v, and the first rate constants for metal alkyl/Ph_3C^+ reactions. Our data provide compelling evidence for prior electron transfer in α-hydride abstraction reactions and strongly suggest a similar pathway for β-hydride abstraction.

Results

I. Characterization of the Electron-Transfer Equilibria. In order to calculate equilibrium constants (K_5) for eq v, the reversible electrode potentials for the half reactions shown in eq vi and vii must be known. From these, K_5 can be calculated by use of the Nernst relationship (eq viii).

$$\mathrm{R{-}(Re)^{\bullet+}} + e^- \overset{E^{\circ}_6}{\rightleftharpoons} \mathrm{R{-}(Re)} \qquad (vi)$$

$$\mathrm{Ph_3C^+} + e^- \overset{E^{\circ}_7}{\rightleftharpoons} \mathrm{Ph_3C^{\bullet}} \qquad (vii)$$

$$\log K_5 = (F/2.303RT)(E^{\circ}_6 - E^{\circ}_7) \qquad (viii)$$

In this study, electrode potentials are obtained by derivative cyclic voltammetry (DCV)[14-16] in $CH_2Cl_2/Bu_4N^+PF_6^-$ (0.1 M) with a platinum disk electrode (d = 0.6 mm) at 208 K.

The DCV response for the oxidation of $PhCH_2$–(Re) (**1**) is given in Figure 1. The positive-going potential sweep is started from

(3) Kiel, W. A.; Lin, G.-Y.; Gladysz, J. A. *J. Am. Chem. Soc.* **1980**, *102*, 3299.

(4) Kiel, W. A.; Lin, G.-Y.; Constable, A. G.; McCormick, F. B.; Strouse, C. E.; Eisenstein, O.; Gladysz, J. A. *J. Am. Chem. Soc.* **1982**, *104*, 4865.

(5) Kiel, W. A.; Lin, G.-Y.; Bodner, G. S.; Gladysz, J. A. *J. Am. Chem. Soc.* **1983**, *105*, 4958.

(6) Merrifield, J. H.; Lin, G.-Y.; Kiel, W. A.; Gladysz, J. A. *J. Am. Chem. Soc.* **1983**, *105*, 5811.

(7) (a) Parshall, G. W. *Homogeneous Catalysis*; Wiley: New York, 1980; pp 16, 39–41, 85–90, 172–173. (b) Kazlauskas, R. J.; Wrighton, M. S. *J. Am. Chem. Soc.* **1982**, *104*, 6005. (c) Turner, H. W.; Schrock, R. R. *Ibid.* **1982**, *104*, 2331. (d) Yang, G. K.; Peters, K. S.; Vaida, V. *Ibid.* **1986**, *108*, 2511.

(8) (a) Hayes, J. C.; Pearson, G. D. N.; Cooper, N. J. *J. Am. Chem. Soc.* **1981**, *103*, 4648. (b) Hayes, J. C.; Cooper, N. J. *Ibid.* **1982**, *104*, 5570. (c) Jernakoff, P.; Cooper, N. J. *Ibid.* **1984**, *106*, 3026. (d) Asaro, M. F.; Cooper, S. R.; Cooper, N. J. *Ibid.* **1986**, *108*, 5193.

(9) Guerchais, V.; Lapinte, C. *J. Chem. Soc., Chem. Commun.* **1986**, 663.

(10) Mandon, D.; Toupet, L.; Astruc, D. *J. Am. Chem. Soc.* **1986**, *108*, 1320.

(11) Bly, R. S.; Bly, R. K.; Hossain, M. M.; Silverman, G. B.; Wallace, E. *Tetrahedron* **1986**, *42*, 1093.

(12) Asaro, M. F.; Bodner, G. S.; Gladysz, J. A.; Cooper, S. R.; Cooper, N. J. *Organometallics* **1985**, *4*, 1020.

(13) See, also: Bodner, G. S.; Gladysz, J. A.; Nielsen, M. F.; Parker, V. D. *Organometallics*, submitted for publication. Although the electrode potentials reported in the previous paper[12] compare favorably with those found in our more detailed study,[13] quantitative DCV and chronoamperometry results indicate that complex **3** undergoes quasi-reversible 1 e$^-$ oxidation, in contrast to previous conclusions.

(14) Ahlberg, E.; Parker, V. D. *J. Electroanal. Chem.* **1981**, *121*, 57, 73.

(15) Parker, V. D. *Adv. Phys. Org. Chem.* **1983**, *19*, 131.

(16) Parker, V. D. *Electroanal. Chem.* **1986**, *14*, 1.

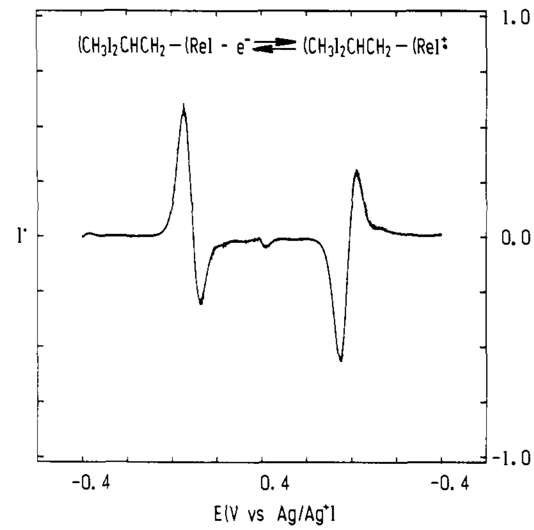

Figure 2. Derivative cyclic voltammogram (DCV) for the oxidation of $(CH_3)_2CHCH_2$–(Re) (**2**) in $CH_2Cl_2/Bu_4N^+PF_6^-$ (0.1 M) at 208 K and 100 mV/s.

a rest potential of −0.3 V (vs. Ag^+/Ag), where no electrode processes take place. The output from the current follower of the potentiostat is routed to an analog differentiator, and the resulting waveform, the first derivative of a cyclic voltammogram, is recorded on a digital oscilloscope. The height of the positive peak, like that in ordinary cyclic voltammetry, is proportional to the substrate concentration. The direction of the potential sweep is reversed at +0.5 V, and the negative peak on this segment is due to the reduction of $\mathbf{1}^{\bullet+}$ in the diffusion layer. The ratio of DCV peak heights on the reverse and forward scans, R'_I, gives a measure of the stability of the electrode-generated intermediate. In Figure 1, R'_I is unity, indicating that $\mathbf{1}^{\bullet+}$ is stable during the time of measurement. The peak potential (E^p) for the oxidation of **1** is defined by the point where the rapidly descending curve passes through zero on the forward scan. Likewise, E^p for the reduction of $\mathbf{1}^{\bullet+}$ is given by the point where the rapidly ascending curve passes through zero on the reverse scan. In practice, the peak potentials are not read from the recordings. Rather, all data are processed by an online computer. It has been demonstrated[17] that precision as high as ±0.1 mV in E^p measurements can be achieved by this procedure.

Providing that all the redox processes to be compared are Nernstian—i.e., are reversible and rapid compared to the time of measurement—the relative peak potentials for the reductions are equivalent to the relative reversible potentials. Although all the redox processes are indeed chemically reversible, none of them fulfill the requirements for Nernstian charge transfer. Therefore, potentials halfway between the forward and reverse peaks of the cyclic voltammograms were taken to be proportional to the reversible potentials for the processes. This is rigorously valid only if the transfer coefficient, α, is equal to 0.5. This is not known to be the case for any of the processes studied, and, therefore, the reversible potential differences obtained must be viewed as approximate. In any event, the error is expected to be no more than a few mV and to give uncertainties in K_5 on the order of 10%.

The DCV response for the oxidation of $(CH_3)_2CHCH_2$–(Re) (**2**) is given in Figure 2. The stability of $\mathbf{2}^{\bullet+}$ is shown by the fact that R'_I is 1.0. Essentially the same result is obtained for the oxidation of (*SR,RS*)-Ph(CH_3)CH–(Re) (**3**). These data show that all three cation radicals R–(Re)$^{\bullet+}$ are long lived in CH_2Cl_2 at 208 K, as predicted from data at higher temperatures.[13]

The DCV response for the reduction of Ph_3C^+ under the same conditions is shown in Figure 3. Here again, R'_I is observed to be 1.0, indicating the high stability of $Ph_3C^\bullet$ under the experimental conditions. In order to gain information on the longer term stability of $Ph_3C^\bullet$, a different approach is used. The rest potential

(17) Eliason, R.; Parker, V. D. *J. Electroanal. Chem.* **1984**, *165*, 21.

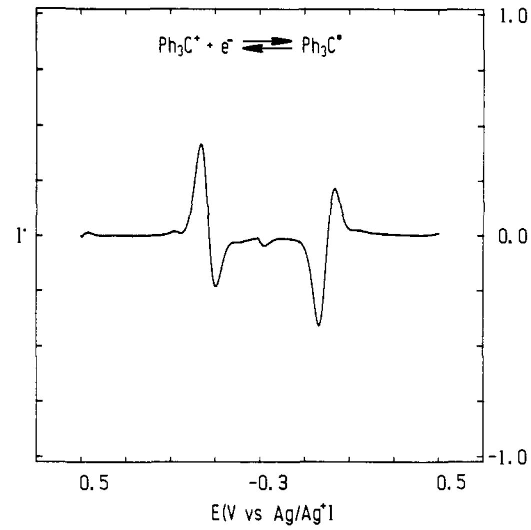

Figure 3. Derivative cyclic voltammogram (DCV) for the reduction of Ph_3C^+ in $CH_2Cl_2/Bu_4N^+PF_6^-$ (0.1 M) at 208 K and 100 mV/s.

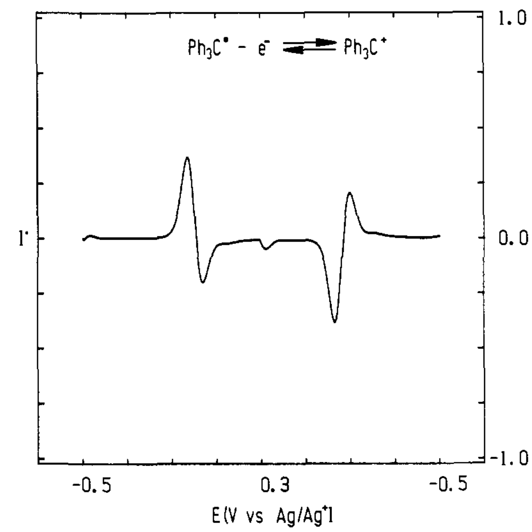

Figure 4. Derivative cyclic voltammogram (DCV) for the oxidation of $Ph_3C^\bullet$ in $CH_2Cl_2/Bu_4N^+PF_6^-$ (0.1 M) at 208 K and 100 mV/s.

Table I. Reversible Electrode Potentials and Equilibrium Data for eq v

substrate (R)	ΔE^p/mV[a]	E_{rev}/mV[b]	K_5
1 ($PhCH_2$)	79	188	2.5×10^{-5}
2 ($(CH_3)_2CHCH_2$)	61	85	7.9×10^{-3}
3 ((Ph)(CH_3)CH)	87	55	5.0×10^{-2}

[a] The potential separation between cyclic voltammetry peaks. Data obtained at 208 K at 100 mV/s on solutions of substrate (1.0 mM) in $CH_2Cl_2/Bu_4N^+PF_6^-$ (0.1 M). [b] The reversible electrode potential referred to $Ph_3C^+ + e^- \rightleftarrows Ph_3C^\bullet$.

of the electrode is made negative of E^p for the reduction of Ph_3C^+ so that the predominant triphenylmethyl species in the diffusion layer is $Ph_3C^\bullet$ (along with some dimer).[18] Under these conditions, DCV gives an indication of even slow reactions of the electrode-generated intermediate. This technique has recently been used to observe transient dimers formed from the 9-diazofluorene anion radical.[19] The DCV response for the oxidation of $Ph_3C^\bullet$ under these conditions is shown in Figure 4. That the peak heights

(18) The dimerization of $Ph_3C^\bullet$ to C_2Ph_6 has been extensively studied. The relative amounts of these two species under our experimental conditions is not presently known. Sholle, V. D.; Rozantsev, E. G. *Russ. Chem. Rev.* **1973**, *42*, 1011. McBride, J. M. *Tetrahedron* **1974**, *30*, 2009. Colle, T. H.; Glaspie, P. S.; Lewis, E. S. *J. Org. Chem.* **1978**, *43*, 2722. Neumann, W. P.; Uzick, W.; Zarkadis, A. *J. Am. Chem. Soc.* **1986**, *108*, 3762.

(19) Bethell, D.; Parker, V. D. *J. Am. Chem. Soc.* **1986**, *108*, 895.

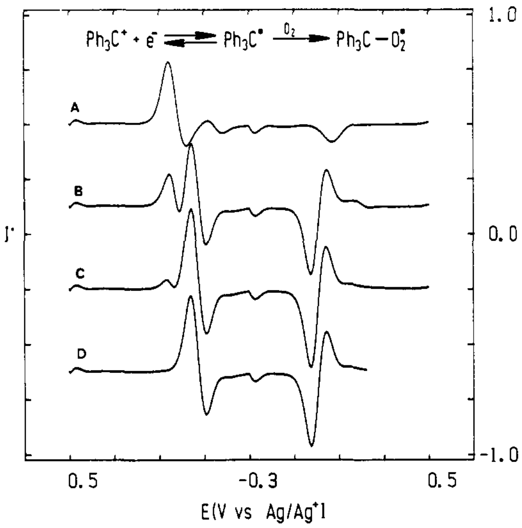

Figure 5. Derivative cyclic voltammograms for the reduction of Ph_3C^+ in $CH_2Cl_2/Bu_4N^+PF_6^-$ (0.1 M) at 208 K and 100 mV/s in the presence of varying concentrations of oxygen. From (A)–(D), the oxygen concentration is lowered by purging with nitrogen.

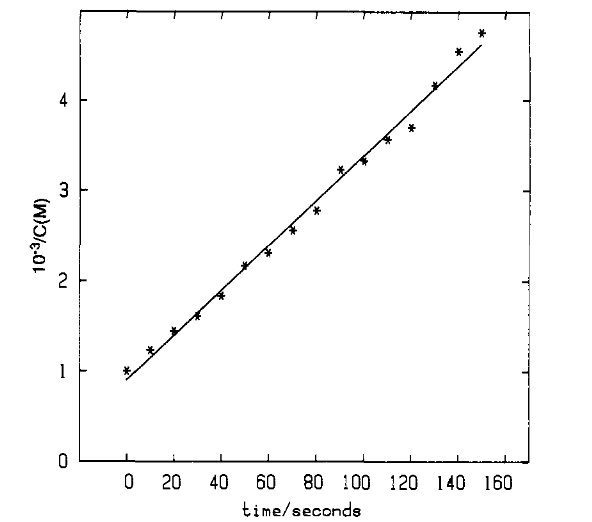

Figure 6. Second-order plot for the depletion of $PhCH_2$–(Re) (**1**) during reaction with equimolar $Ph_3C^+PF_6^-$ (1.0 mM) in $CH_2Cl_2/Bu_4N^+PF_6^-$ (0.1 M) at 208 K under a nitrogen atmosphere. The reaction was monitored by DCV at 10 V/s and 10 s intervals.

are very nearly the same as those in Figure 3 shows that $Ph_3C^•$ is stable under the reaction conditions.

Equilibrium constants for eq v were calculated for all three R–(Re) complexes by using eq viii. The K_5 are listed in Table I and vary by a factor of about 2000.

II. **The Reaction of $Ph_3C^•$ with Oxygen.** A close inspection of Figure 3 reveals a small peak at a potential positive of the Ph_3C^+ reduction peak. It was suspected that this was a prepeak arising from the very rapid reaction of the product of the electrode reaction, $Ph_3C^•$, with some impurity present in concentrations lower than that of the substrate. The origin of such prepeaks has been discussed in terms of a kinetic shift of only a portion of the peak due to substrate when the kinetic process involves insufficient quantities of reactant to consume significant fractions of the electrode-generated intermediate.[20] The rate constant for the follow-up reaction must be very large to observe a prepeak.

In this case, oxygen is a likely candidate to react with $Ph_3C^•$. This would give the triphenylmethylperoxy radical, $Ph_3COO^•$, as shown in equation ix. This was verified by conducting DCV

$$Ph_3C^• + O_2 \xrightarrow{k_9} Ph_3C\text{–O–O}^• \qquad \text{(ix)}$$

measurements on solutions from which the oxygen was intentionally only partially removed. The voltammograms for these experiments are shown in Figure 5. At the highest oxygen concentration (Figure 5A), the entire reduction peak is shifted positively, and there is little indication of the presence of $Ph_3C^•$ on the return scan. This indicates that sufficient oxygen was present to very rapidly react with all $Ph_3C^•$ present in the diffusion layer. Partial depletion of oxygen by purging with nitrogen separates the reduction peaks and allows observation of some $Ph_3C^•$ oxidation on the return scan (Figure 5B). Further depletion of oxygen gives a decrease in the height of the prepeak relative to the main peak and an increase in the height of the peak due to $Ph_3C^•$ oxidation (Figure 5C). The prepeak disappears upon prolonged purging with nitrogen (Figure 5D).

The rate constant for eq ix (k_9) can be evaluated by use of either the shift of the main peak from the reversible one or the difference in potentials between the prepeak and the main peak. Theoretical data are not available for irreversible second-order reactions between two different species for either relationship. However, data are available for the irreversible first-order reaction of the electrode-generated intermediate (commonly referred to as the EC mechanism),[21] and these data can be used to estimate the rate constant. The difference in potentials of the reduction peak in the presence (Figure 5A) and absence (Figure 5D) of oxygen is observed to be 87 mV. Under these conditions ΔE^p, the peak potential separation during cyclic voltammetry for the reduction of Ph_3C^+, is 52 mV. Thus, the quantity required to calculate the rate constant, $E^p - E^{rev}$, is about 61 mV. The concentration of oxygen in the solution used to generate Figure 5A is estimated to be about the same as that of Ph_3C^+, i.e., 1 mM. Thus, we can assume a pseudo-first-order reaction of $Ph_3C^•$ with oxygen with an average concentration of 0.5 mM during the course of recording the reduction peak. This is certainly an approximation but is perhaps not as much as it might seem, since the concentration of $Ph_3C^•$ will be exceedingly small for the very rapid reaction. Making these assumptions, the rate constant can be calculated from eq x, which is valid for the EC mechanism.[21] In eq x, a is

$$(k/a)^{1/2} = \exp((E^p - E^{rev})(F/RT) + 0.78) \qquad \text{(x)}$$

equal to $F\nu/RT$, where F is the Faraday constant, and ν is the sweep rate. This gives a pseudo-first-order rate constant of 2.4×10^4 s^{-1} and a k_9 of 4.8×10^7 M^{-1} s^{-1}. The deviation from pseudo-first-order conditions leads to an underestimate of the rate constant and thus these are minimum values. In any event, it appears safe to conclude that reaction ix is exceedingly rapid and probably very near the diffusion-controlled limit.

III. **Kinetics of Hydride Abstraction.** It was possible to study the kinetics of the reaction of **1** with $Ph_3C^+PF_6^-$ in CH_2Cl_2 at 208 K. Solutions of $Ph_3C^+PF_6^-$ were injected into equimolar solutions of **1** (1:1 reactant ratio), and the reaction was followed by recording DCV scans at 10 V/s at 5 or 10 s intervals. The peak heights were converted to concentrations, and the data were treated according to theory for second-order reactions. Plots of $1/C$ vs. time are shown for reaction under nitrogen (Figure 6) and air (Figure 7). The concentration C refers to **1** in Figure 6 and to $Ph_3C^+PF_6^-$ in Figure 7. The rate constants obtained from the slopes are 24.9 (nitrogen) and 265 (air) M^{-1} s^{-1}. Results of several runs with both **1** and $PhCD_2$–(Re) (**1-d_2**) are summarized in Table

Table II. Second-Order Rate Constants and Deuterium Kinetic Isotope Effect Data for the Reactions of $PhCH_2$–(Re) (**1**) and $PhCD_2$–(Re) (**1-d_2**) with $Ph_3C^+PF_6^-$

atmosphere[a]	k_{app}/M^{-1} s^{-1} [b]	k_H/k_D
nitrogen	22.5 ± 2.4	5.4 ± 0.5
air	240 ± 51	1.0 ± 0.2

[a] Equimolar concentrations (1.0 mM) of reagents in CH_2Cl_2 mixed at 208 °C. Reaction monitored by analyzing DCV scans recorded at 5- or 10-s intervals. [b] The apparent second-order rate constant for the reaction of **1** with $Ph_3C^+PF_6^-$, evaluated as the slope of plots of $1/C$ vs. t.

(20) Jensen, B. S.; Parker, V. D. *Electrochim. Acta* **1973**, *18*, 665.
(21) Nicholson, R. S.; Shain, I. *Anal. Chem.* **1964**, *36*, 706.

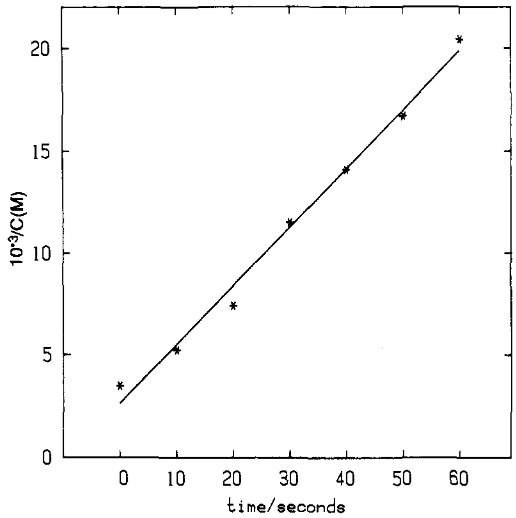

Figure 7. Second-order plot for the depletion of $Ph_3C^+PF_6^-$ during reaction with equimolar $PhCH_2$–(Re) (**1**) (1.0 mM) in $CH_2Cl_2/Bu_4N^+PF_6^-$ (0.1 M) at 208 K under an atmosphere of air. The reaction was monitored by DCV at 10 V/s and 10 s intervals.

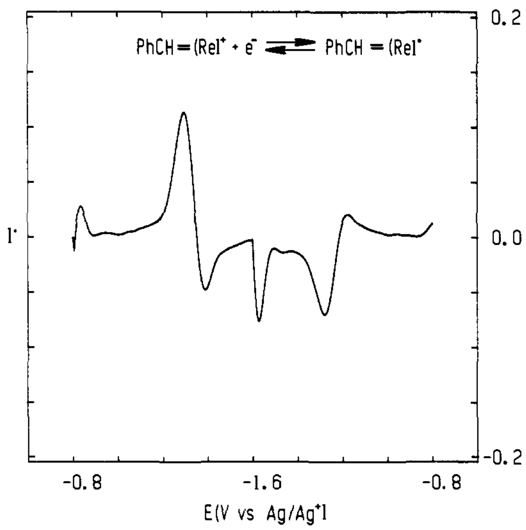

Figure 8. Derivative cyclic voltammetry (DCV) analysis of *sc*-PhCH=(Re)$^+$ produced during reaction of equimolar $PhCH_2$–(Re) (**1**) and Ph_3C^+ PF_6^- (1.0 mM) in $CH_2Cl_2/Bu_4N^+PF_6^-$ (0.1 M) at 208 K under nitrogen. Recorded at 10 V/s immediately after transferring the reaction to a 293 K bath.

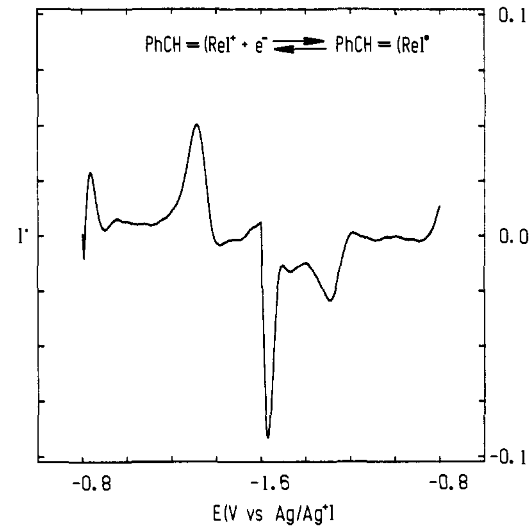

Figure 9. Derivative cyclic voltammetry (DCV) analysis of *sc*-PhCH=(Re)$^+$ produced during reaction of equimolar $PhCH_2$–(Re) (**1**) and Ph_3C^+ (1.0 mM) in $CH_2Cl_2/Bu_4N^+PF_6^-$ (0.1 M) at 208 K under air. Recorded at 10 V/s immediately after transferring the reaction to a 293-K bath.

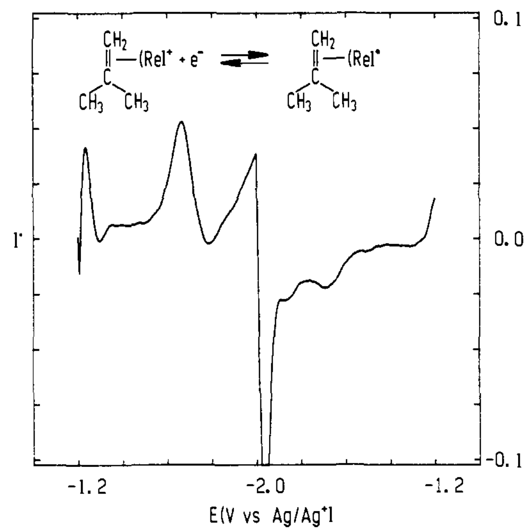

Figure 10. Derivative cyclic voltammetry (DCV) analysis of $((CH_3)_2C{=}CH_2)$–(Re)$^+$ produced during reaction of equimolar $(CH_3)_2CHCH_2$–(Re) (**2**) and $Ph_3C^+PF_6^-$ (1.0 mM) in $CH_2Cl_2/Bu_4N^+PF_6^-$ (0.1 M) at 208 K under nitrogen. Recorded at 10 V/s at 293 K.

II. The rates of the reactions conducted in air are so rapid as to be near the upper limit for which kinetic measurements can be made by the technique used. The limiting factors are the rate of mixing and the time necessary to carry out and analyze the DCV scan. The maximum rate of data sampling possible was found to be about 5 s/point. Thus, data for the runs carried out in air are subject to greater errors than for the slower runs under nitrogen. The data give a kinetic isotope effect, k_H/k_D, of 5.4 $\pm$ 0.5 for the runs under nitrogen and 1.0 $\pm$ 0.2 for the runs under air.

It was not possible to obtain analogous rate constants for **2** and **3**, since the oxidation peaks of $Ph_3C^\bullet$ and R–(Re) and the reduction peaks of Ph_3C^+ and R–(Re)$^{\bullet+}$ overlapped. The reactions of both **2** and **3** appear to be considerably faster than that of **1**. This is based upon the qualitative observation of the rate of disappearance of the overlapped DCV peaks for the oxidation of $Ph_3C^\bullet$ and R–(Re) after mixing the reactants at 208 K.

IV. Products Derived from Rhenium. Although the products of the above reactions have been well-characterized,[4,5] it was desirable to verify their formation, especially for the experiments conducted in the presence of oxygen. An authentic sample of the more stable Re=C isomer of the alkylidene complex derived from **1**, *ac*-PhCH=(Re)$^+$, underwent reduction during cyclic voltammetry in $CH_2Cl_2/Bu_4N^+PF_6^-$ (0.1 M) with a peak potential of ca. −1.3 V.[22] The initial product obtained from the reaction of **1** and $Ph_3C^+PF_6^-$ under nitrogen, which is expected to be the less stable alkylidene Re=C isomer, *sc*-PhCH=(Re)$^+$, was characterized by the voltammogram shown in Figure 8. The yield was shown to be greater than 80% by comparing the peak height with that of *ac*-PhCH=(Re)$^+$. Product characterization was slightly more difficult for reactions carried out in the presence of oxygen. The height of the peak due to the reduction of *sc*-PhCH=(Re)$^+$ changed rapidly with time and completely disappeared within 20–30 min, indicating reaction with oxygen or reaction byproducts. The voltammogram shown in Figure 9 was recorded shortly after warming to room temperature and indicates about a 40% yield of product remaining.

The alkene complex derived from **2**, $((CH_3)_2C{=}CH_2)$–(Re)$^+$, was reduced with a peak potential close to −1.7 V. The product from reaction of **2** with $Ph_3C^+PF_6^-$ under nitrogen gave the

(22) Unavoidable drift in the reference electrode was encountered in the reaction mixtures, so exact potentials were not measured. The identities of the peaks were verified by additions of authentic compounds.

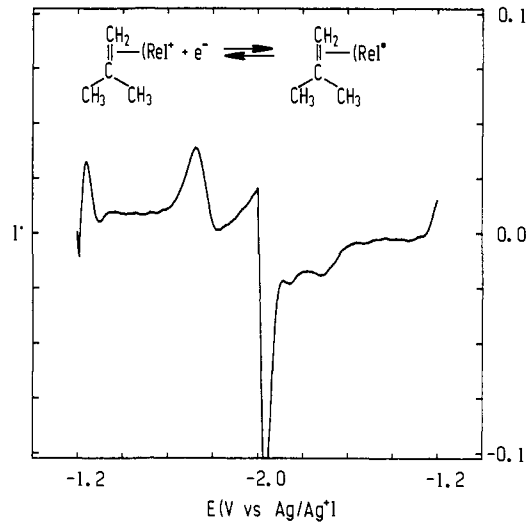

Figure 11. Derivative cyclic voltammetry (DCV) analysis of $((CH_3)_2C{=}CH_2)$-(Re)$^+$ produced during reaction of equimolar $(CH_3)_2CHCH_2$-(Re) (**2**) and $Ph_3C^+PF_6^-$ (1.0 mM) in $CH_2Cl_2/Bu_4N^+PF_6^-$ (0.1 M) at 208 K under air. Recorded at 10 V/s at 293 K.

voltammogram shown in Figure 10. In this case, $((CH_3)_2C{=}CH_2)$-(Re)$^+$ was not observed until the solution had warmed to room temperature, and then the signal intensity increased with time.[23] The analogous reaction conducted in the presence of oxygen behaved similarly, but the product peak disappeared after about 1 h. The reduction peak height on the voltammogram recorded (Figure 11) was about 70% of that in Figure 10. A preparative reaction of $(CH_3)_2CHCD_2$-(Re) (**2-d_2**)[5] and $Ph_3C^+PF_6^-$ was conducted under air (CH_2Cl_2, -78 °C) to ensure that oxygen did not affect the hydride abstraction regiochemistry. The β-hydride abstraction product $((CH_3)_2C{=}CD_2)$-(Re)$^+$, which mass spectral (FAB) and ^{1}H NMR analysis showed to be >98% d_2, was isolated in 44% yield after workup at room temperature.[24]

We suspect that the initial yields of rhenium complexes are very similar for the reactions carried out under nitrogen and air, but we were unable to show this experimentally because of further reactions in the oxygen containing solutions. However, even under these circumstances we were able to show that the yields under air are at least 40–70% of those under nitrogen.

V. Products Derived from $Ph_3C^+PF_6^-$. Gas liquid chromatography (GLC) was used to analyze the products derived from $Ph_3C^+PF_6^-$. Data are summarized in Table III. In addition to the product normally obtained, Ph_3CH, significant amounts of benzophenone, PhCOPh, were observed. The most plausible route for the formation of benzophenone is the decomposition of the hydroperoxide Ph_3COOH as in eq xi.[25] This is a common reaction, possibly occurring during GLC analysis, and was not characterized further.

$$Ph_3C\text{-}O\text{-}O\text{-}H \rightarrow PhCOPh + PhOH \qquad \text{(xi)}$$

(23) This reaction was also studied by both ^{1}H and ^{31}P NMR spectroscopy. By ^{1}H NMR, a 66% yield (relative to $Ph_3P^+CH_2C_6H_5PF_6^-$ internal standard) of $((CH_3)_2C{=}CH_2)$-(Re)$^+$ was observed 0.5 h after mixing the reactants in CD_2Cl_2 at -80 °C. The yield increased to 88% upon warming the sample to room temperature. Starting material appeared to be consumed at -80 °C, but we have previously noted that when *less* than 1 equiv of $Ph_3C^+PF_6^-$ is added to alkyl complexes R-(Re) at -78 °C, ^{1}H spectra can misleadingly show all of the alkyl complex to be consumed, presumably due to the generation of paramagnetic cation radicals R-(Re)$^{\bullet+}$ and subsequent electron exchange.[5] These results were qualitatively confirmed by ^{31}P NMR monitoring, which showed some starting material (broadened resonance) remaining at -80 °C.

(24) The potential α-hydride abstraction product $(CH_3)_2CHCH{=}$(Re)$^+$ would rearrange to $((CH_3)_2C{=}CH_2)$-(Re)$^+$ at 10–25 °C: Hatton, W. G.; Gladysz, J. A. *J. Am. Chem. Soc.* **1983**, *105*, 6157. Hence, α-hydride abstraction from **2-d_2** would have given the d_1 product $((CH_3)_2C{=}CHD)$-(Re)$^+$. We thank a reviewer for suggesting the possibility of a change in hydride abstraction regiochemistry under oxygen, which prompted this experiment.

(25) Nonhebel, D. C.; Tedder, J. M.; Walton, J. C. *Radicals*; Cambridge Press: Cambridge, 1979; Chapter 14.

Table III. Organic Products from Reactions of $Ph_3C^+PF_6^-$ with R-(Re)[a]

run	substrate (*R*)	atmosphere	yields[b] % PhCOPh	yields[b] % Ph_3CH
1	**1** ($PhCH_2$)	air	70.7 (4.0)	3.8 (1.0)
2	**1** ($PhCH_2$)	air	63.8 (2.0)	1.4 (1.0)
3[c]	**1** ($PhCH_2$)	air	45.4 (1.3)	2.4 (0.5)
4	**1** ($PhCH_2$)	nitrogen	5.3 (0.9)	82.3 (4.1)
5	**1** ($PhCH_2$)	nitrogen	4.6 (0.2)	83.0 (2.8)
6	**2** ($(CH_3)_2CHCH_2$)	air	64.9 (4.6)	7.2 (1.2)
7	**2** ($(CH_3)_2CHCH_2$)	air	64.9 (2.3)	5.5 (1.7)
8	**2** ($(CH_3)_2CHCH_2$)	air	73.4 (3.6)	5.9 (1.4)
9	**2** ($(CH_3)_2CHCH_2$)	nitrogen	14.4 (2.6)	66.6 (2.0)
10	**2** ($(CH_3)_2CHCH_2$)	nitrogen	13.4 (1.0)	62.4 (3.1)

[a] Reactions carried out on equimolar (2.0 mM) solutions in CH_2Cl_2 at 208 K. [b] Yields assuming a 1/1 stoichiometry. The numbers in parentheses are the standard deviations for at least three replicate measurements. [c] In this run, a small amount of active alumina was added in an attempt to settle finely divided insoluble particles, and absorption may have decreased the PhCOPh yield.

There is a noteworthy effect of the nature of the rhenium–alkyl complex upon the distribution of products derived from $Ph_3C^+PF_6^-$. The yields of benzophenone, under either air or nitrogen, are about three times greater for $(CH_3)_2CHCH_2$-(Re) (**2**) than for $PhCH_2$-(Re) (**1**).

Discussion

I. Mechanism. In the previous section, we presented thermodynamic, kinetic, and product distribution data on the reactions of $Ph_3C^+PF_6^-$ with a series of rhenium–alkyl complexes. All of our findings are consistent with a common mechanism involving an electron-transfer preequilibrium followed by a rate-determining, product-forming, hydrogen-atom transfer between radical species produced during electron transfer or in a subsequent reaction. The mechanism is summarized in eq xii–xv with $PhCH_2$-(Re) (**1**) as an example.

$$\underset{\mathbf{1}}{PhCH_2\text{-(Re)}} + Ph_3C^+ \underset{k_{-12}}{\overset{k_{12}}{\rightleftharpoons}} PhCH_2\text{-(Re)}^{\bullet+} + Ph_3C^\bullet \qquad \text{(xii)}$$

$$Ph_3C^\bullet + PhCH_2\text{-(Re)}^{\bullet+} \xrightarrow{k_{13}} Ph_3C\text{-H} + PhCH{=}\text{(Re)}^+ \qquad \text{(xiii)}$$

$$Ph_3C^\bullet + O_2 \xrightarrow{k_{14}} Ph_3C\text{-O-O}^\bullet \qquad \text{(xiv)}$$

$$Ph_3C\text{-O-O}^\bullet + PhCH_2\text{-(Re)}^{\bullet+} \xrightarrow{k_{15}} Ph_3C\text{-O-O-H} + PhCH{=}\text{(Re)}^+ \qquad \text{(xv)}$$

The evidence, which we will show to be consistent with this mechanism and to rule out plausible alternatives, is comprised of the following observations: (1) $Ph_3C^\bullet$ and all R-(Re)$^{\bullet+}$ studied are stable when generated separately under conditions of the hydride abstraction reactions. The values of K_5 observed at 208 K, 2.5×10^{-5}–5.0×10^{-2}, predict sufficient concentrations of radical intermediates to account for the reaction kinetics. (3) $Ph_3C^\bullet$ and oxygen react at a nearly diffusion-controlled rate, and the radical is effectively trapped by reaction with oxygen. (4) The major organic product derived from $Ph_3C^+PF_6^-$ in the absence of oxygen is Ph_3CH, but in the presence of oxygen is benzophenone, arising from Ph_3COOH. (5) The products derived from R-(Re) appear to be independent of whether the reactions are carried out in the presence or absence of oxygen. (6) The second-order rate constant for the reaction between $PhCH_2$-(Re) (**1**) and $Ph_3C^+PF_6^-$ is increased by an order of magnitude when oxygen is present. (7) A significant deuterium kinetic isotope effect is observed for the reactions of $PhCH_2$-(Re) (**1**) and $PhCD_2$-(Re) (**1-d_2**) with $Ph_3C^+PF_6^-$ in the absence of oxygen but not in the presence of oxygen.

II. Stability of Radical Intermediates. All cation radicals R-(Re)$^{\bullet+}$ appear to be stable in CH_2Cl_2 at 208 K. Thermal decomposition occurs very slowly at room temperature, and with relatively high activation energies, of the order of 10 kcal/mol.[13]

Alkylidene or alkene complexes are not produced. This requires that an electron-transfer mechanism for the hydride abstraction reaction consists of two steps, eq xii and xiii.[26]

The DCV shown in Figure 4 indicates a remarkable stability for $Ph_3C^\bullet$ under the reaction conditions. The rest potential of the electrode is −0.5 V, where all Ph_3C^+ reaching the electrode is transformed to the radical. Thus, the predominant species in the diffusion layer is $Ph_3C^\bullet$, along with the dimer,[18] under these conditions. Since the peak height for the oxidation is very nearly the same as for the reduction of Ph_3C^+ when the rest potential was +0.5 V (Figure 3), the lifetime of the radical must be expressed in minutes. The chlorine atoms of CH_2Cl_2 are readily abstracted by reactive radicals.[27] Since $Ph_3C^\bullet$ reacts so slowly with the CH_2Cl_2 solvent, if at all, under the reaction conditions, it is not a potent atom abstraction agent. This indicates that in order for eq xiii to occur rapidly, the carbon–hydrogen bond must be activated to a high degree by the cation–radical metal center.

III. Implications Arising from the Electron-Transfer Equilibria Data. Of the reactions studied, that of **1** and $Ph_3C^+PF_6^-$ is the least favorable for electron transfer. The relative values of K_5 for **1**/**2**/**3** are found to be 1:316:2000. Thus, if it can be demonstrated that the electron-transfer mechanism for hydride abstraction is energetically feasible for **1**, then it must be even more so for the other substrates.

It seems reasonable to assume that the thermodynamically favorable electron-transfer reaction, the reverse of eq xii, takes place near the diffusion-controlled limit under these conditions. This assumption, $k_{-12} = k_{diff}$, allows an estimate of the forward electron-transfer rate constant (k_{12}) from the appropriate K_{12} and the diffusion-controlled rate constant (k_{diff}) under the reaction conditions by using eq xvi. With k_{diff} equal to 5×10^8 M^{-1} s^{-1}

$$k_{12} = k_{diff}K_{12} \qquad \text{(xvi)}$$

(see discussion below) and K_{12} (equal to K_5) equal to 2.5×10^{-5}, this results in $k_{12} = 1.25 \times 10^4$ M^{-1} s^{-1}. Thus, according to this estimate a second-order reaction involving eq xii as the rate-determining step could have a rate constant as great as 1.25×10^4 M^{-1} s^{-1}. The observed rate constant is 22.5 M^{-1} s^{-1} in the absence of oxygen and 240 M^{-1} s^{-1} in the presence of oxygen. Thus, the estimated value of k_{12} could be as much as two orders of magnitude too great and still be consistent with the electron-transfer mechanism. It would appear that the electron-transfer mechanism for the hydride abstraction reaction is energetically feasible for all R–(Re) studied.

IV. Trapping of $Ph_3C^\bullet$ with Oxygen. The chemical trapping of reactive intermediates is a common means of obtaining evidence for their participation in reactions.[28] The trapping of $Ph_3C^\bullet$ with oxygen during the reduction of Ph_3C^+ is clearly demonstrated by the DCV response shown in Figure 5. As discussed earlier, the rate constant for reaction ix, k_9, can be estimated directly from the voltammetric data to be equal to about 5×10^7 M^{-1} s^{-1}.

In connection with this reaction as well as for the discussion in the previous section it is of interest to estimate the value of k_{diff} (the diffusion-controlled second-order rate constant) for reactions under the experimental conditions of this study. Activation energies for diffusion of a number of compounds in aprotic solvents have been determined from voltammetric measurements.[29] It was suggested that k_{diff} can be calculated from the absolute rate equation by substituting $(E_a)_{diff}$, the diffusion activation energy, for the enthalpy of activation. This gives eq xvii. Taking an

$$\ln k_{diff} = \ln \frac{ekT}{h} - (E_a)_{diff}/RT + \Delta S^\ddagger{}_{diff}/R \qquad \text{(xvii)}$$

average value of $(E_a)_{diff}$ found for the solvents used, 2.5 kcal/mol, and the average $\Delta S^\ddagger{}_{diff}$ (entropy of activation for diffusion) found, −7.9 cal/K mol, gives $k_{diff} = 5 \times 10^8$ M^{-1} s^{-1}. Keeping the approximations involved in the treatment in mind, this can be used as a rough estimate for the diffusion-controlled rate constant under the conditions of the hydride ion abstraction reactions.

These considerations suggest that k_9 (= k_{14}) is within about an order of magnitude of k_{diff}. In terms of the mechanism for hydride abstraction, this suggests that if reaction xii is essentially in equilibrium in the absence of oxygen, this will not necessarily be the case when $Ph_3C^\bullet$ is trapped by oxygen. The rate enhancement observed, roughly an order of magnitude, in the presence of oxygen could either be due to reaction xii becoming irreversible and the rate control shifting to k_{12} or to the larger rate constant for reaction xv, k_{15}, than for reaction xiii, k_{13}. The two possibilities are readily distinguished by the deuterium kinetic isotope effect studies with $PhCH_2$–(Re) (**1**) and $PhCD_2$–(Re) (**1**-d_2). As predicted from the discussion above, a significant deuterium kinetic isotope effect is observed when the reactions are carried out under nitrogen. However, there is no difference within experimental error (±21%) in rate constants measured for analogous reactions in the presence of oxygen. The latter does indeed indicate a change in the rate-determining step for the reactions carried out in the presence of oxygen and suggests that under these conditions the rate is controlled by the electron transfer shown in eq xii. Significantly, appreciable deuterium kinetic isotope effects were also observed (competition experiments) in reactions of $Ph_3C^+PF_6^-$ with CH_3CH_2–(Re) and CH_3CD_2–(Re) (α-hydride abstraction) and (*SS*,*RR*)-$Ph(CH_3)CH$–(Re) and (*SS*,*RR*)-$Ph(CD_3)CH$–(Re) (β-hydride abstraction) under nitrogen.[5]

No data are available regarding the relative rates of reactions xiii and xv. It is, however, very likely that reaction xv is considerably more rapid than reaction xiii. The carbon–hydrogen bond dissociation energy of Ph_3C–H is 75 kcal/mol,[30] while the oxygen–hydrogen bond dissociation energy in R–O–O–H is about 90 kcal/mol.[25] This suggests that reaction xv is probably more exothermic than reaction xiii. The reaction of R–O–O$^\bullet$ with C–H is the key step in auto-oxidation reactions,[25] and these can be exceedingly rapid. On the other hand, $Ph_3C^\bullet$ appears to be stable in the presence of a relatively good atom donor, CH_2Cl_2. It appears to be justified to assume that reaction xv is significantly more rapid than reaction xiii.

V. Implication of the Product Distributions. Importantly, the rhenium-containing products appear to be the same and formed in comparable yields regardless of whether reactions are conducted in the presence or absence of oxygen. At the same time, a drastic change takes place in the distribution of organic products derived from $Ph_3C^+PF_6^-$.

The fact that in the presence of oxygen the major product becomes benzophenone, which is readily formed from Ph_3COOH, suggests that reaction xv is the principal route to organic products under these conditions. It is difficult to find any alternative to reaction xv to produce Ph_3COOH. Under the reaction conditions, Ph_3CH does not react with oxygen at a significant rate. Thus, the product distribution implicates electron-transfer equilibrium (eq v) when reactions are conducted in the presence of oxygen. Although we cannot rule out the possibility from our data, it seems highly unlikely that there is a mechanism change in the presence of oxygen—i.e., that in the absence of oxygen the reaction takes place by the abstraction of hydride ion from R–(Re) as shown in eq xviii for **1**. This possibility would suggest that the Ph_3CH

$$Ph_3C^+ + \underset{\mathbf{1}}{PhCH_2\text{–}(Re)} \rightarrow Ph_3C\text{–}H + PhCH{=}(Re)^+ \qquad \text{(xviii)}$$

formed during the reactions in the presence of oxygen arises from competing reaction xviii. There is an indication that this is unlikely. Since K_5 (electron transfer to Ph_3C^+) is 316 times greater for **2** than **1**, the competing reaction scheme would suggest that there should be much less Ph_3CH formed from **2**. The results

(26) A reviewer has raised the possibility of a three-step, $-e^-/-H^+/-e^-$, hydride-transfer mechanism. We find no reaction between cation radicals $R\text{–}(Re)^{\bullet+}$ and pyridine and hence consider this pathway unlikely.

(27) Bridger, R. F.; Russell, G. A. *J. Am. Chem. Soc.* **1963**, *85*, 3765.

(28) Isaacs, N. S. *Reactive Intermediates in Organic Chemistry*; Wiley: London, 1974.

(29) Aalstad, B.; Parker, V. D. *Acta Chem. Scand.* **1982**, *B36*, 295.

(30) Lloyd, W. G. In *Methods in Free Radical Chemistry*; Huyser, E. S., Ed.; Dekker: New York, 1973; Vol. 4, Chapter 1.

show the opposite trend; about 3 times more Ph_3CH is produced with **2** than with **1**.

We also considered the possibility that hydride abstraction takes place by an electron-transfer-initiated chain mechanism consisting of eq xii or eq v in the general case, followed by chain propagating steps as shown in eq xix and xx. This mechanism is indeed an

$$Ph_3C^{\bullet} + PhCH_2\text{–(Re)} \rightarrow Ph_3C\text{–H} + PhCH\text{=(Re)}^{\bullet} \quad \text{(xix)}$$

$$PhCH\text{=(Re)}^{\bullet} + Ph_3C^{+} \rightarrow PhCH\text{=(Re)}^{+} + Ph_3C^{\bullet} \quad \text{(xx)}$$

alternative, and we cannot rule it out. It seems likely that the $R\text{–(Re)}^{\bullet+}$, a higher energy species, is more susceptible to attack by $Ph_3C^{\bullet}$ than is neutral R–(Re). On the other hand, eq xix and xx constitute simply an alternative description of the electron-transfer mechanism, differing only in which species takes part in the hydrogen atom transfer and is not kinetically distinguishable from the other formulation.

VI. Conclusions. We interpret our data in terms of an electron-transfer preequilibrium followed by a hydrogen atom transfer to yield the observed hydride abstraction products. Cooper and co-workers have used chemical data to demonstrate an analogous pathway for α-hydride abstraction from tungsten–alkyl complexes $(\eta^5\text{-}C_5H_5)_2W(CH_3)(CH_2R)$ by $Ph_3C^+PF_6^-$.[8] Interestingly, in this system the electron transfer is exothermic, and radical cations $[(\eta^5\text{-}C_5H_5)W(CH_3)(CH_2R)]^{\bullet+}$ can be isolated under appropriate conditions. Guerchais and Lapinte have used ESR to detect cation radical intermediates in the abstraction of an α-hydride from iron–hydroxymethyl complex[9] $(\eta^5\text{-}C_5Me_5)Fe(CO)_2(CH_2OH)$ by $Ph_3C^+PF_6^-$. We further suggest that available mechanistic data on other Ph_3C^+/metal alkyl reactions are consistent with this pathway.[31]

On the basis of the above discussion, it is possible but unlikely that eq xviii is a significant competing reaction. An alternative formulation of the electron-transfer mechanism involves hydrogen atom transfer from R–(Re) and electron transfer (eq xx) as propagating steps in a chain reaction. We feel that this is less likely on the basis of the expected relative reactivities of R–(Re) and $R\text{–(Re)}^{\bullet+}$ in the hydrogen atom transfer.

Finally, it can be inferred that properties of cation radicals $R\text{–(Re)}^{\bullet+}$ (or species that are formed in rapid subsequent steps) must determine the regiochemistry of the hydride abstraction reactions shown in eq ii–iv. These cation radicals are the subject of ongoing study in our laboratories.

Experimental Section

The instrumentation, data handling procedures, cells, and electrodes were similar to those described in previous publications.[14,32]

All reactions were carried out in reagent grade CH_2Cl_2 that had been passed through a column of active neutral alumina before use to remove water and protic impurities. The $Ph_3C^+PF_6^-$ was precipitated from a minimum amount of CH_2Cl_2 with ethyl acetate and washed with ethyl acetate before use. Complexes **1–3** were prepared as described previously.[4,5]

Homogeneous kinetic studies were carried out by injecting a 1.0 mM CH_2Cl_2 solution of $Ph_3C^+PF_6^-$ into an equal volume of a 208 K, 1.0 mM CH_2Cl_2 solution of R–(Re) in a bath controlled by a Haake cryostat. The concentrations of reactants were monitored by DCV scans at 10 s intervals controlled by a Hewlett Packard HP 3314A function generator interfaced to a Hewlett Packard 9825 desk computer. The DCV scans were recorded on a Nicolet 2090 digital oscilloscope and processed with the desk computer.

For organic product analysis, reactions were carried out as above but with reactants that were 2.0 mM (total volume 5.0 mL). The solutions were kept at 208 K for 5 min and then warmed to room temperature. The solvent was removed under a stream of N_2, and an equivalent amount of anthracene standard in CH_2Cl_2 (1.0 mL) was added. The organometallic products were precipitated with hexane (10 mL), and analysis of the supernatant was conducted on a Perkin Elmer 3920B gas chromatograph (210 °C, 2 m 10% S.E. 30 column) equipped with a Hewlett Packard HP 3380S electronic integrator. Retention times (min) and relative response factors (average of three measurements: mmol/mL): benzophenone, 3.3, 0.934 ± 0.01; anthracene, 5.8, 1.00; Ph_3CH, 11.3, 1.39 ± 0.03.

Acknowledgment. We gratefully acknowledge support from the Norsk Hydro Fund (M.F.N.; administered by the Norwegian Institute of Technology) and the U.S. Department of Energy (G.S.B., J.A.G).

Registry No. 1, 71763-28-5; **2**, 85926-73-4; **2** (α-d_2), 74540-81-1; **3**, 82374-39-8; *ac*-$PhCH\text{=(Re)}^+PF_6^-$, 74561-64-1; *sc*-$PhCH\text{=(Re)}^+PF_6^-$, 74540-78-6; $((CH_3)_2C\text{=}CH_2)(Re)^+PF_6^-$, 85926-83-6; $((CH_3)_2C\text{=}CD_2)(Re)^+PF_6^-$, 106682-23-9; $Ph_3P^+PF_6^-$, 437-17-2; O_2, 7782-44-7; D_2, 7782-39-0.

(31) Hannon, S. J.; Traylor, T. G. *J. Org. Chem.* **1981**, *46*, 3645.

(32) Ahlberg, E.; Parker, V. D. *Acta Chem. Scand.* **1980**, *B34*, 97.